https://doi.org/10.2352/ISSN.2470-1173.2021.16.COLOR-244

Determining Optimal Resolution for Scanned Document Raster Content*

Zhenhua Hu[1], Peter Bauer[2], Todd Harris[2], Jan Allebach[1]
[1]School of Electrical and Computer Engineering, Purdue University, West Lafayette, Indiana, 47907
[2]HP Inc., Boise, Idaho, 83714

Abstract

Modern scan routines require a predefined scan resolution, whether it is customer-selected or a default value in the scanner's settings. When the scanning process begins, the resolution cannot be changed. This results in all scanned pages, no matter how much their contents may vary, having output images of the same size. If we can determine an optimal resolution for each scanned document raster content, we can save a lot of storage. In this paper, the resolutions in question are 300 dpi, 150 dpi, and 75 dpi. We define the criteria for optimal scan resolution and propose some new features to help determine it for scanned document raster content. The features proposed are sample power spectrum mean squared error (MSE), edge density, and edge contrast. These features can reflect the truthfulness between high-resolution 300 dpi images (references) and their low-resolution (150 dpi and 75 dpi) counterparts and the intrinsic changes among them. Combining them with spatial activity, tile standard deviation (STDDEV) structural similarity index measure mean (tile-STDDEV SSIM), and tile STDDEV structural similarity index measure STDDEV (tile-STDDEV SSIM STDDEV), we can form a feature vector, which is then fed into an SVM classifier. Test result shows that we can achieve a prediction accuracy of 93.4%.

Introduction

Currently, when scanning documents using automatic document feeders (ADFs), people need to define a scan resolution, or use the default setting in the scanner. After the scanning process begins, the resolution cannot be changed. This makes the resulting scanned images have the same resolution, and the same size if saved as uncompressed files. But this can lead to inefficient usage of memory, especially for document pages containing different raster contents, as shown in Figure 1. Although they look very different, the two pages will have the same size using the current scanning process. But we can clearly see that the flat image in Figure 1a only needs a scan resolution of 75 dpi, but the line drawing in Figure 1b requires 300 dpi to keep all details. If we set the scan resolution to be 75 dpi, we will lose a lot of information in Figure 1b. If the scan resolution is 300 dpi, storing scanned version of Figure 1a will need much more storage than needed.

In order to solve this problem, we need to determine the optimal scan resolution according to the scanned document raster content. Here, optimal scan resolution refers to the lowest scan resolution that keeps all details in the scanned copy. In this paper, the resolutions in question are 300 dpi, 150 dpi, and 75 dpi. We choose 300 dpi as the highest scan resolution because after looking at many scanned images from 600 dpi to 75 dpi, we think that 300 dpi is good enough to keep all details of the scanned documents. We choose 75 dpi as the lowest scan resolution because it is the smallest value in most HP scanners. 150 dpi is added into consideration because it is half of 300 dpi, and twice of 75 dpi. To the best observation of the author, it is also commonly used in everyday scanning processes. To decide the optimal resolution for a scan document raster content, we need to compare the image quality across 300 dpi, 150 dpi, and 75 dpi, and choose the lowest resolution that has all the information as the 300 dpi version can provide.

(a) Flat image (b) Line drawing

Figure 1: Example of two pages with different contents. We can see that picture (a) contains a plain area, while picture (b) has more detail. So we can see that they need different scan resolutions.

Image quality (IQ) or image quality assessment (IQA) is a widely-studied topic and many quality estimators (QEs) have been developed [1][2]. Based on whether a reference image exists or how complete the reference image is, QEs can be divided into three categories: full-reference (FR), reduced reference (RR), and no reference (NR) QEs. FR QEs are developed by taking into consideration a perfect reference image. Examples are mean squared error (MSE) or peak signal-to-noise ratio (PSNR), most apparent distortion (MAD) [3], structural similarity index (SSIM) [4][5], and visual information fidelity (VIF) [6]. They all require the reference images of the same size. RR QEs are used in cases where reference images are available, but too costly to get. Examples include "divisive normalization" [7] and "quality-aware image"

*Research supported by HP Inc., Boise ID 83714

QEs [8]. Often they are based on natural scene statistics (NSS) models [9]. NR QEs are used in cases where no reference images are available. They instead exploit the intrinsic properties of test images. Examples are edge raggedness [10][11], small speckles [12][13], blocking [14][15], ringing [16], sharpness [17][18], or features based on deep neural networks [19].

Since the reference 300 dpi images are much larger than the test images of 150 dpi and 75 dpi resolution, we cannot use the FR QEs mentioned above. There are also studies that can assess image quality across different resolutions, like the Multiscale Image Quality Estimator (MIQE) [20], which is used to assess images of different resolutions from various viewing devices like laptops, televisions, and smart phones. A cross spatial resolution image QE [21] was proposed to estimate the quality of interpolated high-resolution images compared to their low-resolution counterparts. But both QEs do not consider the fact that since the scanned images are stored in the same device, people may zoom in a low-resolution image for better viewing experience. Thus, in the scope of FR QEs, comparing the image quality between the 300 dpi reference image and the resized 150 dpi and 75 dpi images is more similar to people's viewing habits.

In this paper, we propose a method to determine the optimal scan resolution for different scanned raster contents. We develop one FR QE: sample power spectrum MSE, and some NR QEs (edge density and edge contrast). Along with spatial activity [22], tile standard deviation (STDDEV) structural similarity index measure mean (tile-STDDEV SSIM), and tile STDDEV structural similarity index measure STDDEV (tile-STDDEV SSIM STDDEV) [23], we can have a feature vector for a scanned page. After collecting feature vectors for a large self-created dataset, we can feed them into an SVM classifier for training and testing. Experiments show that we can have a prediction accuracy of 93.4%.

Methodology

Sample Power Spectrum MSE

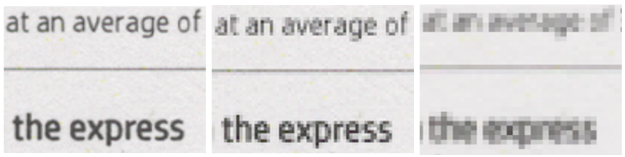

(a) Reference 300 dpi image (b) Resized 150 dpi image (c) Resized 75 dpi image

Figure 2: Changes of scanned character images from 300 dpi to 75 dpi. For a better viewing experience, the lower resolution images are resized to the same size as that of 300 dpi through nearest-neighbor interpolation.

With the decrease of the scan resolution, we can clearly see the loss of details, such as the blurring of edges, as shown in Figure 2, which indicates the changes from 300 dpi to 150 dpi and then to 75 dpi images. Note that the 150 dpi and 75 dpi images are resized to the same size of 300 dpi through the nearest-neighbor interpolation. We choose this resizing method because after studying common image and pdf viewing software, we found that the results of nearest-neighbor interpolation method resembles closely the resizing effects of these software tools. We can see that the characters are clearly distinguishable when scanned at 300 dpi. Although we can identify the words in the resized 150 dpi image, the small-sized words in the top are a little bit blurry. The situation is even worse in the resized 75 dpi image, as the characters seem to have merged together, and it becomes impossible to tell the words.

The detail changes from 300 dpi to 150 and 75 dpi images indicate the sample power spectrum changes. Thus, we can calculate the sample power spectrum mean squared error (MSE) of (300 dpi, 150 dpi) and (300 dpi, 75 dpi) image pairs as one QE. Note that in order to most resemble the human viewing habits, we need to resize 150 dpi and 75 dpi images to the size of 300 dpi reference images before calculating the power spectrum MSE.

Edge Density

Perhaps the most obvious changes we can notice with the decrease of the scan resolution is that images are getting more and more blurry. For some document images and line drawings with very close but distinct edges, one or more close edges may be hard to distinguish or even merge into one when the scan resolution decreases from 300 dpi to 75 dpi. This would cause some of the characters to become unidentifiable, and drawings to lose information. With this motivation in mind, we define a new NR QE: edge density, that can take the changes of both the foreground and background pixels into consideration, and thus better reflect the local pixel changes.

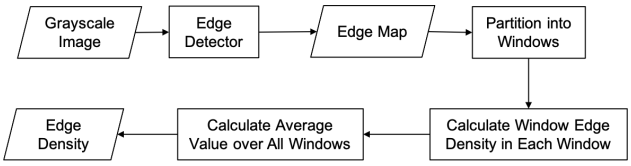

Figure 3: Workflow to calculate edge density.

Figure 3 shows the workflow to calculate edge density. Color images are converted to grayscale before being passed into the workflow. Then we apply the Canny edge detector [25] to get the edge map, on which we calculate the edge density. In order to be able to capture small changes, we partition the edge map into small windows. In order to assure the pixel correspondences and window numbers from different scan resolutions, we choose different window sizes according to their resolutions. Then window edge density values are calculated in each window, and we take the average value as the edge density of the image.

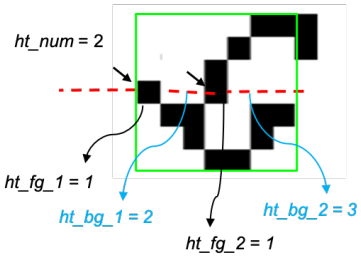

Figure 4: An example of horizontal edge density.

The edge density is comprised of two parts: horizontal edge density and vertical edge density. Figure 4 shows an example of how we compute horizontal edge density. The process is as follows:

(1) Imagine a horizontal line (the red dashed line in Figure 4) passing through the center of the small window (the green box).

(2) Count the number of horizontal transitions along the horizontal line. A transition is defined as sudden change from *background* to *foreground*. In this case, the number of horizontal transitions ht_num is 2.

(3) Following the horizontal line, count the number of consecutive foreground pixels, and then the number of consecutive background pixels, and then the number of consecutive foreground pixels, and so on. In this case, the numbers are 1, 2, 1, 3, denoted in the figure as ht_fg_1, ht_bg_1, ht_fg_2, ht_bg_2, respectively. In Figure 4, the number of consecutive foreground and background pixels are color-coded as black and blue, respectively. Note that the smallest number of foreground or background pixels is 1, since the counting process is based on pixels, and one pixel belongs either to the foreground or the background.

(4) The horizontal edge density $ht\_density$ is calculated using the formula

$$ht\_density = ht\_num \cdot \left(\sum_{i}^{I} \mathbb{1}(ht\_fg\_i > 0) \frac{1}{ht\_fg\_i} + \sum_{j}^{J} \mathbb{1}(ht\_bg\_j > 0) \frac{1}{ht\_bg\_j} \right) \tag{1}$$

where $\mathbb{1}$ is the indicator function. I is the total number of sequences of foreground pixels, and J is the total number of sequences of background pixels. ht_fg_i is the number of consecutive foreground pixels in the i-th sequence of foreground pixels, and ht_bg_j is the number of consecutive background pixels in the j-th sequence of foreground pixels. Their values are all larger than 0. In Figure 4, the horizontal edge density is $2 \cdot (1/1 + 1/2 + 1/1 + 1/3) = 5.67$.

The reason why we sum the reciprocals of consecutive foreground/background pixel numbers is that it can better reflect the merging of foreground/background line segments. Clearly, image quality degrades most when foreground and background pixels are interleaved by one pixel. Namely, one foreground pixel is followed by one background pixel, and then followed by one background pixel, and so on. In this situation, simply downsampling the image from 300 dpi to 150 dpi would make the resultant image lose a lot of information. With large pixel numbers, like a 10-pixel-width foreground line segment followed by a 10-pixel-width background segment, the image quality would not be affected much even when downsampled to 75 dpi. As a result, we use the reciprocals of line segments to reflect drastic changes in the number of foreground and background pixels.

The vertical density is calculated in a similar way, as shown in Figure 5. We draw a vertical line through the window center, and count the number of consecutive foreground and background pixels. The equation to calculate the vertical edge density $vt\_density$ is

$$vt\_density = vt\_num \cdot \left(\sum_{i}^{I} \mathbb{1}(vt\_fg\_i > 0) \frac{1}{vt\_fg\_i} + \sum_{j}^{J} \mathbb{1}(vt\_bg\_j > 0) \frac{1}{vt\_bg\_j} \right) \tag{2}$$

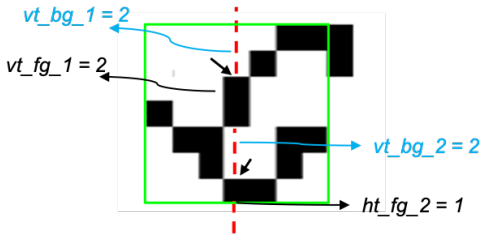

Figure 5: An example of vertical edge density.

where $\mathbb{1}$ is the indicator function. I is the total number of sequences of foreground pixels, and J is the total number of sequences of background pixels. vt_num is the number of vertical transitions. vt_fg_i is the number of consecutive foreground pixels in the i-th sequence of foreground pixels along the vertical line, and vt_bg_j is the number of consecutive background pixels in the j-th sequence of foreground pixels. Their values are all larger than 0. In Figure 5, the horizontal edge density is $2 \cdot (1/2 + 1/2 + 1/2 + 1/1) = 5$.

Clearly, the direction that would achieve the maximum edge density value is the most vulnerable to suffer from changes in scan resolution. So the final edge density $edge\_density$ is

$$edge\_density = max(vt\_density,\ ht\_density) \tag{3}$$

Accordingly, the edge density for the window shown in Figure 4 and Figure 5 is $max(5.67,\ 5) = 5.67$

Edge Contrast

Blurry edges are the most apparent quality degradation when the scan resolution goes down from 300 dpi to 75 dpi. The separated edges merged together. Some areas with high frequency alternation between black and white become gray. Although the edge density can reflect the merging of edges, they cannot represent the changes of pixel values around edges. Those pixel value changes around edges are important since they reflect the contrast, which is a very important QE. As a result, we propose a QE based on Michelson contrast [24].

Contrast is the difference in color or intensity that makes an object distinguishable from its surrounding background. The human visual system (HVS) is more sensitive to contrast than absolute intensity; and this enables us to see a world similarly despite the big intensity changes from day to night. Since Michelson contrast is easy to calculate, and takes into consideration both the maximum and minimum intensity values. We choose it to calculate the contrast changes from 300 dpi to 150 and 75 dpi images.

Michelson contrast is defined as

$$c\_michelson = \frac{I_{max} - I_{min}}{I_{max} + I_{min}} \tag{4}$$

where *c_michelson* is the Michelson contrast. I_{max} and I_{min} are the maximum and minimum intensity values, respectively, of the areas in question.

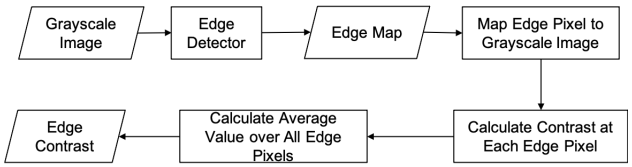

Figure 6: Workflow to calculate edge contrast.

Figure 6 shows the workflow to calculate edge contrast. Since it is a NR QE, we only need one input image. Color images are converted to grayscale before being fed into the pipeline. We use the Canny edge detector [25] to detect edges since it can result in 1-pixel-width edge maps. After getting the edge pixels, we map them back to the grayscale image. Specifically we will use the coordinates of edge pixels in the edge map to identify the edge pixels in the grayscale image, and to calculate the Michelson contrast in a small window. The window sizes are based on the scan resolutions (shown in Table 1); so that the calculated contrast values correspond to roughly the same area, independent of the resolution of the image.

Table 1: Scan resolutions and their corresponding window size.

Resolution (dpi)	Window width/height (pixel number)
300	13
150	7
75	3

Spatial Activity

In the paper [22], the spatial activity is defined as the root mean square (RMS) difference between the edge maps of two images. The color images are turned into grayscale before calculating the spatial activity. Since this is a FR feature, we also need to resize the low-resolution image to the size of the high-resolution image through nearest-neighbor interpolation.

Tile-STDDEV SSIM

Tile-STDDEV SSIM and Tile-STDDEV SSIM STDDEV [23] are introduced as QEs to assess image qualities of different scan resolutions. The idea is that the input images are first partitioned into the same number of tiles by selecting tile sizes proportional to the scan resolutions. Then, the standard deviation (STDDEV) of each tile is calculated, and forms a tile STDDEV map. Since all resolution images have the same number of tiles, their resultant tile maps have the same size. Based on these tile maps, Tile-STDDEV SSIM and Tile-STDDEV SSIM STDDEV are calculated. Results in [23] show that they can effectively reflect image quality changes with the decrease of scan resolutions.

Data Collection

We collect our own data for training and testing. In this paper, we mainly focus on line drawings and cartoon images. The collection process follows the routine below.

(1) PDF files are collected from the internet, and printed using an HP LaserJet 500 color MFP M575.

(2) Pages are scanned into 300 dpi digital images using HP Officejet Enterprise Color Flow MFP X585 with the HP-internal *w_scan* routine. *W_scan* is chosen instead of regular scanning because it does not include post-processing steps like edge enhancement and JPEG compression, which may unnecessarily affect our judgement.

(3) In order to augment the data set, the 300 dpi images are partitioned into 300 pixel $\times$ 300 pixel sub-images. Duplicated sub-images are removed. Each sub-image is treated separately as an individual image. In this paper we do not consider stitching the sub-images together. We also rotate the sub-images for data augmentation. We do not use flipping because most of our features are flipping-invariant.

(4) Images of other resolutions are achieved from 300 dpi sub-images using area-based downsampling instead of scanning to save processing time.

Optimal scan resolution is quite an ambiguous term. Although we can understand it as the lowest scan resolution with acceptable image quality, we still need to make it clear what the acceptable image quality is. In the scope of this paper, we define two criteria for acceptable image quality:

(1) For 75 dpi and 150 dpi images, we resize them to the size of their 300 dpi counterpart. Since blurriness and jaggedness are two most obvious degradations in our scope (Figure 7). The blurriness or jaggedness is either imperceptible, or perceptible but not annoying in the resized image. Clearly, this is a NR criterion, as we do not need a reference image.

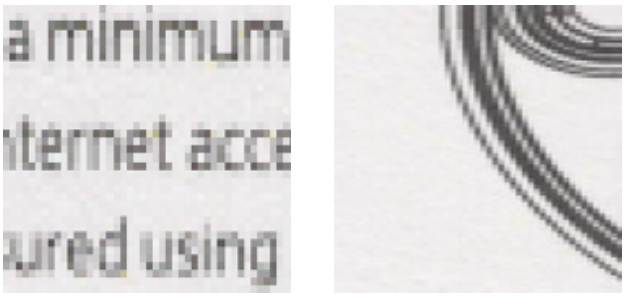

(a) Blurriness (b) Jaggedness

Figure 7: Examples of blurriness and jaggedness.

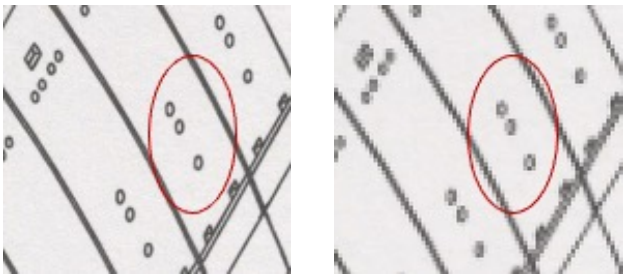

(a) 300 dpi image (b) Resized low-resolution image

Figure 8: An example of detail loss. We can clearly see three circles in the red oval in (a). But in the same area of (b), we are not very sure if they are circles.

(2) If we resize the low-resolution image to the size of the 300 dpi reference, the resized image must contain all the details that the reference image contains. For example, if there is a circle in the 300 dpi image, there must be also a circle (not a square, or not sure if it is a circle or square) in the resized image, as is shown in Figure 8.

Figure 9 shows the workflow of how we label the optimal scan resolution for a sub-image. The high-resolution image is the 300 dpi reference image, and the low-resolution images are 150 dpi and 75 dpi images. Here, 300 dpi images are captured through scanning, and low-resolution images are generated using the area-based downsampling method to save processing time. The low-resolution (150 dpi and 75 dpi) images are resized by nearest-neighbor interpolation to the same size as that of their 300 dpi reference image. All images, the reference image, and the two resized images are opened in the same image viewing software, at 100% of image size. The viewer then looks at the three images side by side, and picks the optimal scan resolution based on the criteria mentioned above. All sub-images are viewed on a 14-inch HP Elitebook 840 G3 laptop. The display resolution is 1366 pixels $\times$ 768 pixels. The subject was seated straight in front of the laptop, with the laptop slightly below the eye height. The distance between the laptop and the subject's eyes is around three times the height of the laptop screen. The subject is asked to wear glasses or contact lenses if needed. For the work reported in this paper, the author was only subject.

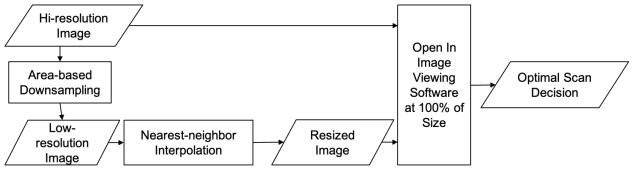

Figure 9: Workflow to label optimal scan resolution. Each low-resolution (150 dpi and 75 dpi) image is resized to the same size as that of its 300 dpi reference image. The reference image and both of the resized images are opened in the same image viewing software. Finally, the optimal resolution for the input image is chosen.

The resolutions and their corresponding number of scanned sub-images collected are shown in Table 2. For each resolution, we have 537 sub-images and the data set has in total $1,611$ sub-images. These sub-images are generated from 45 scanned whole pages.

Table 2: Ground truth optimal scan resolution and the number of sub-images

Scan Resolution	No. of Sub-Images
300 dpi	537
150 dpi	537
75 dpi	537
Overall	**1,611**

Experimental Results

After getting the features, we use an SVM to train and test the accuracy of our model. In practice, we use LIBSVM [26] with a radial basis function (RBF) as the kernel, to execute the training and testing process. LIBSVM uses grid search, and is very efficient in finding the optimal parameters. In order to get a more compelling result, we use 5-fold cross-validation to test our model. Precisely, we split the training data equally into five folders. For each experiment, we pick four of them as the training set to get the SVM model, and the remaining one folder as the testing set to get the testing accuracy. We repeat this process four times, each time with a different folder as the testing set. The final accuracy is the average of all five experiments. We also test the training accuracy by running the model on the training data.

Table 3 shows the training and cross-validation results. We see that we achieve a training accuracy of 95.2%, and validation accuracy of 93.4% with a STDDEV of 1.2%.

Table 3: Training and validation results.

	Accuracy	STDDEV
Training	95.2%	0.3%
Cross-validation	93.4%	1.2%

Conclusion

Current scanning mechanisms scan all pages into the same resolution, which may cause an inefficient use of storage. To tackle this problem, we first define a criteria based on which to judge an image's quality. That is, when resized to the same size as that of 300 dpi, the blurriness or jaggedness is either imperceptible, or perceptible but not annoying in the resized image. Also, the resized image should keep all the details that its 300 dpi reference image has. The resolution that meets both criteria is called the optimal scan resolution. Then we propose some new QEs: sample power spectrum MSE, edge density, and edge contrast. We combine them with spatial activity, tile-STDDEV SSIM, and tile-STDDEV SSIM STDDEV. Concatenating these features and feeding them into an SVM, we can have a prediction accuracy of 93.4%.

Acknowledgement

The image used in Figure 1b is designed by Vectorpocket / Freepik. The whole project is supported by HP Inc. in Boise, Idaho. We really appreciate their help.

References

[1] A. C. Bovik, "Automatic prediction of perceptual image and video quality," *Proc. IEEE*, vol. 101, no. 9, pp. 2008–2024, 2013.

[2] K. Seshadrinathan and A. C. Bovik, "Automatic prediction of perceptual image and video quality," *Proc. IEEE*, vol. 101, no. 9, pp. 2008–2024, 2013.

[3] E. C. Larson and D. M. Chandler, "Most apparent distortion: Full-reference image quality assessment and the role of strategy," *J. Electron. Imaging*, vol. 19, no. 1, p. 011006, 2010.

[4] Z. Wang, A. C. Bovik, H. R. Sheikh, and E. P. Simoncelli, "Image quality assessment: From error visibility to structural similarity," *IEEE Trans. Image Process.*, vol. 13, no. 4, pp. 600–612, 2004.

[5] R. Szeliski, "Computer vision: Algorithms and applications," *Springer Sci. Bus. Media*, 2010.

[6] H. R. Sheikh and A. C. Bovik, "Image information and visual quality," *IEEE Trans. Image Process.*, vol. 15, no. 2, pp. 430–444, 2006.

[7] Q. Li and Z. Wang, "Reduced-reference image quality assessment using divisive normalization-based image representation," *IEEE J. Selected Topics Signal Process.*, vol. 3, no. 2, pp. 202–211, 2009.

[8] Z. Wang, G. Wu, H. R. Sheikh, E. Simoncelli, E. Yang, and A. C. Bovik, "Quality-aware images", *IEEE Trans. Image Process.*, vol. 15, no. 5, pp. 1680–1689, 2006.

[9] R. Soundararajan and A. C. Bovik, "RRED indices: Reduced reference entropic differencing for image quality assessment," *IEEE Trans. Image Process.*, vol. 21, no. 2, pp. 517–526, 2011.

[10] J. Grice and J. P. Allebach, "The print quality toolkit: An integrated print quality assessment tool," *J. Imaging Sci. Technol.*, vol. 43, no. 2, pp. 187–199, 1999.

[11] L. Zhang, A. Veis, R. Ulichney, and J. Allebach, "Binary text image file preprocessing to account for printer dot gain," in *IEEE Int. Conf. Image Process. (ICIP)*, pp. 2639–2643, 2014.

[12] M. Cannon, J. Hochberg, and P. Kelly, "Quality assessment and restoration of typewritten document images," *Int. J. Document Anal. Recognition*, vol. 2, no. 2-3, pp. 80–89, 1999.

[13] H. Li, and D.S. Doermann, "Text quality estimation in video," in *Document Recognition Retrieval IX, Int. Society Opt. Photonics*, vol. 4670, pp. 232-243, 2001.

[14] F. Pan, X. Lin, S. Rahardja, W. Lin, E. Ong, S. Yao, Z. Lu, and X. Yang, "A locally adaptive algorithm for measuring blocking artifacts in images and videos," *Signal Process., Image Commun.*, vol. 19, no. 6, pp. 499–506, 2004,

[15] A. C. Bovik and S. Liu, "DCT-domain blind measurement of blocking artifacts in DCT-coded images," in 2001 IEEE Int. Conf. Acoustics, Speech, Signal Process. Proceedings (Cat. No. 01CH37221), vol. 3, pp. 1725–1728, 2001.

[16] X. Feng and J. P. Allebach, "Measurement of ringing artifacts in JPEG images," in *Digital Publishing, Int. Society Opt. Photonics*, vol. 6076, p. 60760A, 2006.

[17] N. Nayef and J.-M. Ogier, "Metric-based no-reference quality assessment of heterogeneous document images," in *Document Recognition Retrieval XXII, Int. Soc. Opt. Photonics*, vol. 9402, p. 94020L, 2015.

[18] B. Zhang, J. P. Allebach, and Z. Pizlo, "An investigation of perceived sharpness and sharpness metrics," in *Image Quality Syst. Performance II, Int. Soc. Opt. Photonics*, vol. 5668, pp. 98–110, 2005.

[19] H. Li, F. Zhu, and J. Qiu, "DeepITQA: Deep based image text quality assessment," in *Int. Conf. Neural Inform. Process.*, Springer, pp. 397–407, 2018.

[20] A. M. Demirtas, A. R. Reibman, and H. Jafarkhani, "Full-reference quality estimation for images with different spatial resolutions," *IEEE Trans. Image Process.*, vol. 23, no. 5, pp. 2069–2080, 2014.

[21] H. Yeganeh, "Cross dynamic range and cross resolution objective image quality assessment with applications," *UWSpace*, 2014. [Online]. Available: http://hdl.handle.net/10012/8667.

[22] P. G. Freitas, W. Y. Akamine, and M. C. Farias, "Using multiple spatio-temporal features to estimate video quality," *Signal Process. Image Commun.*, vol. 64, pp. 1–10, 2018.

[23] Z. Hu, L. Hu, P. Bauer, T. Harris, and J. Allebach, "Relation between image quality and scan resolution: Part I," in *Image Quality Syst. Performance XVII, (Part of IS&T Electron. Imaging 2020)*, vol. no. 9, pp.322–1, 2020.

[24] A. Michelson, "Studies in optics," *U. Chicago Press, IL*, 1927.

[25] J. Canny, "A computational approach to edge detection," *IEEE Trans. Pattern Anal. Mach. Intell.*, no. 6, pp. 679–698, 1986.

[26] C.-C. Chang and C.-J. Lin, "LIBSVM: A library for support vector machines," *ACM Trans. Intelligent Syst. Technol.*, vol. 2, 27:1–27:27, 2011, Software available at http: //www.csie.ntu.edu.tw/ cjlin/libsvm.

Author Biography

Zhenhua Hu received his BS in biomedical engineering from the Shandong University (2011) and his MS in biomedical engineering from Zhejiang University (2014). Currently, he is a Ph.D. candidate at Purdue University. His research focuses are image processing, computer vision, and image quality.

JOIN US AT THE NEXT EI!

IS&T International Symposium on

Electronic Imaging

SCIENCE AND TECHNOLOGY

Imaging across applications . . . Where industry and academia meet!

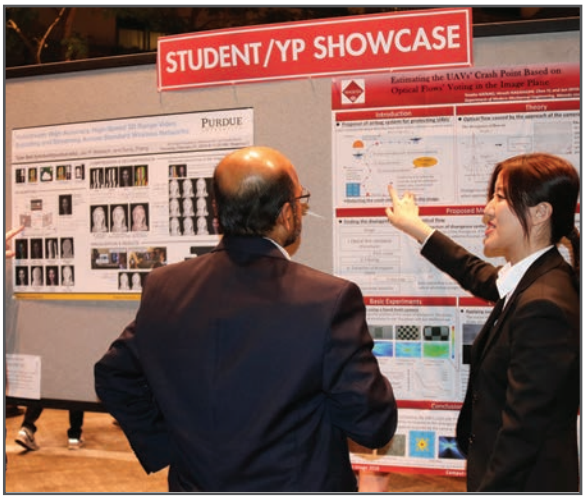

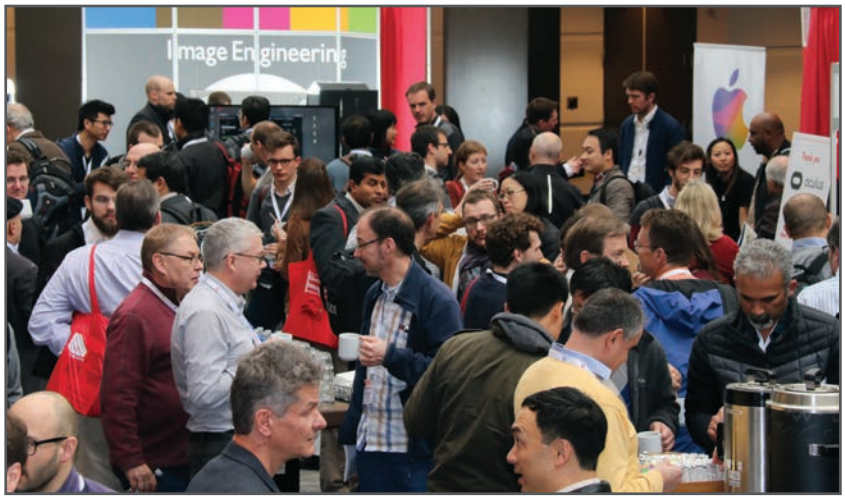

• SHORT COURSES • EXHIBITS • DEMONSTRATION SESSION • PLENARY TALKS •
• INTERACTIVE PAPER SESSION • SPECIAL EVENTS • TECHNICAL SESSIONS •

www.electronicimaging.org

IS&T
imaging.org